Journal of Engineering Mathematics, Vol. 4, No. 2, April 1970
Wolters-Noordhoff Publishing–Groningen
Printed in the Netherlands

On the Critical Point of the Crocco–Lees Mixing Theory in the Laminar Near Wake

D. K. AI*

Geophysical Technology Corporation, Pasadena, California, USA

(Received April 30, 1969)

SUMMARY

The application of the multimoment integral method to the study of the base pressure behind a supersonic vehicle is examined. The primary purpose is to understand the exact nature of the Crocco–Lees critical point, which provides a uniqueness condition in the problem. The analysis is carried out mainly in Poincaré phase space, where the singularities of the differential equations are investigated. Two singular curves are found. The one which is physically meaningful for the near wake flow is located downstream of the rear stagnation point. This singular curve consists of saddle points which yield "wake" solutions, and focal points or saddle-foci. Only those saddle points which yield "wake" solutions correspond to Crocco–Lees critical points. Thus, the integration of the differential equations should be started from a saddle point both for the upstream and the downstream solutions. The current analysis then requires that one deal with only a one-parameter (freestream Mach number) family of solutions, rather than the two-parameter (freestream Mach number and Reynolds number based on thickness of the viscous shear layer at the rear stagnation point) family of solutions obtained in previous works. Finally, this paper clarifies anomalous details of previous numerical investigations carried out for the near wake by Webb, Golik, Vogenitz, and Lees.

Nomenclature

a_{ij}	See Eq. (11)
C_i	See Eq. (11)
C_{ij}	See Eq. (14)
D	See Eq. (12)
F_1, F_2	See Eqs. (17a) and (17b)
f	See Eq. (7)
M_δ	Local Mach number at the edge of the shear layer
M_∞	Freestream Mach number
N_i	See Eq. (12)
p	Pressure
R_∞	Freestream Reynolds number based on the thickness of the shear layer at the rear stagnation point taken as unity
R_{∞_e}	Equivalent freestream Reynolds number
R_{∞_m}	Minimum freestream Reynolds number
u	Velocity component parallel to axis
v	Velocity component normal to axis
U	Dimensionless velocity ratio
U_o	Dimensionless velocity ratio evaluated on the axis
x, y	Cartesian coordinates parallel and normal to axis, respectively
x_1, x_2, x_3	Dependent variables of the governing differential equations, see Eq. (11)
β	See Eq. (7)
γ	Specific heat ratio, equals 1.4
δ	Physical thickness of the viscous shear layer
δ^*	Displacement thickness of the viscous shear layer
ε	Enthalpy ratio $=(1+\frac{1}{2}(\gamma-1)M_\delta^2)^{-1}$
ζ	Independent variable of the governing equations

* Former Member of Technical Staff, Aerosciences Laboratory, TRW Systems, Rendondo Beach, California, USA.

ξ, η	Transformed coordinates transverse and normal to axis, respectively
λ	Characteristic roots of the set of the linear equations (Eq. 15) which describes the behavior of the singularities
μ	Viscosity coefficient
ν	Normalized transformed normal coordinate, see Eq. (10)
ρ	Density
ϕ	Angle of inclination of the inviscid flow at the edge of the viscous shear layer measured positive in the clockwise sense, see Eqs. (3) and (5)
ω	Prandtl–Meyer relation

Subscripts

i	Condition of the flow at the rear stagnation point
i, j	Cartesian tensor indices
c	Condition at the critical point
δ	Condition at the edge of the viscous shear layer
∞	Freestream condition

1. Introduction

Much attention has been focused on the calculation of the base pressure behind a supersonic vehicle at zero angle of attack. Crocco and Lees [1] pointed out over a decade ago that "mixing" between the viscous region near the axis of the wake and the inviscid outer region is very important in establishing the properties of the base flow. Using boundary layer equations to describe the viscous region, these authors showed that in order to determine uniquely a physically meaningful solution, the integral curves of the viscous conservation equations must go through a downstream saddle-point-type singularity. This mathematical singularity has become known as the Crocco–Lees "critical point"; the physical interpretation of this critical point is that the flow undergoes a transition from one which is subsonic in the mean (or subcritical) to one which is supersonic in the mean (or supercritical). The original mixing theory of Crocco and Lees, however, required the introduction of an empirical relation to complete the formulation so that all the unknowns could be determined. By applying multimoment integrals to the boundary layer equations, Reeves and Lees [2] finally removed the need for empirical data. Furthermore, with the aid of Stewartson's [3] reverse flow profile, the solution upstream of the rear stagnation point showed the characteristics of a recirculation region. However, the theory did not give a satisfactory prediction of the distance over which the pressure rises from the base value (the pressure behind the vehicle after the flow has expanded around the base) to the downstream maximum value (the over-shoot pressure produced by the compression which turns the converging wake flow back parallel to the axis). Webb, Golik, Vogenitz and Lees [4] improved the prediction of the pressure recovery distance by introducing a modified Stewartson profile with one higher-moment equation. In addition, Webb *et al.* tried a polynomial velocity profile and found that although the Stewartson profile provided better results upstream of the rear stagnation point, the polynomial profiles led to almost identical results downstream of the stagnation point.

One also observes that in Refs. 1, 2 and 4, the "body" which produces the base flow has never been included in the analysis; thus the only meaningful physical length in the problem appears to be the thickness of the shear layer at the rear (or wake) stagnation point. In Fig. 1, a sketch of the flow field under consideration is shown; the origin of the physical coordinates x, y is located at the rear stagnation point.

In both the work of Reeves and Lees and of Webb *et al.*, the problem was treated as an initial-value one, and the initial condition was taken as the condition at the rear stagnation point. Since the location of the critical-point singularity was not known *a priori*, the problem became one of finding, by trial and error, those initial conditions that permitted the integral curves to pass through the singular point.

In the work by Webb *et al.*, the problem became fully specified when the values of two independent parameters were given. The first parameter was the freestream Mach number M_∞ and the second one, the freestream Reynolds number R_∞, based on the initial thickness of the shear layer. The need for this second parameter obviously arose from the fact that the initial value of the shear layer thickness must be prescribed in order to fully specify the problem.

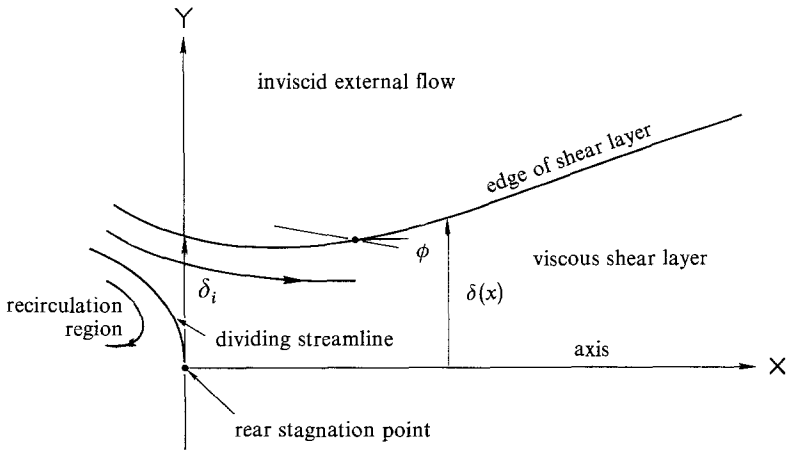

Fig. 1. Schematic of the flow in the neighborhood and downstream of the rear stagnation point.

One, therefore, dealt with a two-parameter family of solutions. In their numerical investigation, they further discovered that for a fixed M_∞, there existed a minimum freestream Reynolds number R_{∞_m} such that for $R_\infty < R_{\infty_m}$ no solution could be found. The most severe case occurred when the total enthalpy of the flow is conserved (adiabatic flow); e.g., for $M_\infty = 6$, R_{∞_m} became as large as 2×10^4 for both the Stewartson and polynomial velocity profiles. When the flow was very cold (non-adiabatic), R_{∞_m} decreased to as low as 0.8×10^4. Also, unexpectedly, for $R_\infty > R_{\infty_m}$ two acceptable initial conditions existed.* The second initial condition occurred at a much higher initial Mach number and was, therefore, taken to be physically unrealistic. Nonetheless, it furnished a perfectly acceptable solution for the problem in a formal mathematical sense. This discovery seemed to indicate a possible non-uniqueness of solution inherent in the differential equations adopted to describe the physical phenomenon. The same non-uniqueness appeared in the numerical solution of the near wake obtained by Baum and Denison [5] using finite-difference methods.

In the present paper, an attempt is made to examine critically the multimoment method used by Webb *et al.* The following items are investigated:

1. The location and nature of the singularities of the differential equations;
2. the conditions under which a "wake solution" exists; and
3. all the possible solutions of the equations which pass through such saddle-point singularities as are found to exist.

The present analysis also shows that the differential equations depend on only one parameter, the freestream Mach number; consequently, the solutions form a one-parameter family. This point will be expanded upon below when integration of the equations starting from the saddle-point singularity (rather than from the rear stagnation point) is suggested.

In order to bring out the essential features of the analysis without unnecessarily tedious algebra, the author has elected to treat only the polynomial velocity profiles for the adiabatic case. Also, it is convenient to carry out a major portion of the analysis in Poincaré phase space.

2. Multimoment Integrals and the Velocity Profiles

In the following treatment all symbols and definitions are identical with those adopted in [4]. The boundary layer approximations are applied to the viscous shear layer, which is assumed

* Private communication from Dr. R. Golik of TRW Systems.

to be a two-dimensional compressible adiabatic flow. The governing equations are:

$$\frac{\partial(\rho u)}{\partial x} + \frac{\partial(\rho v)}{\partial y} = 0 \tag{1}$$

$$\rho u \frac{\partial u}{\partial x} + \rho v \frac{\partial u}{\partial y} = -\frac{dp}{dx} + \frac{\partial}{\partial y}\left(\mu \frac{\partial u}{\partial y}\right). \tag{2}$$

The external flow field is taken to obey the Prandtl–Meyer relation. If we denote ϕ as the angle of inclination of a streamline entering the edge of the viscous layer (see Fig. 1) then (see [4])

$$\phi = \omega - \omega_\infty \tag{3}$$

and

$$\omega = \left(\frac{\gamma+1}{\gamma-1}\right)^{\frac{1}{2}} \tan^{-1}\left[\frac{2-(\gamma+1)\varepsilon}{(\gamma+1)\varepsilon}\right]^{\frac{1}{2}} - \tan^{-1}\left[\frac{2(1-\varepsilon)}{(\gamma-1)\varepsilon} - 1\right]^{\frac{1}{2}} \tag{4}$$

where $\varepsilon = (1+\frac{1}{2}(\gamma+1)M_\delta^2)^{-1}$ is the enthalpy ratio written in terms of the local Mach number at the edge of the boundary layer. In order to make the inviscid flow field compatible with the viscous region, one must satisfy an overall continuity relation (see [1])

$$\tan\phi = -\frac{v_\delta}{u_\delta} = (\delta - \delta^*)\frac{d}{dx}\ln \rho_\delta u_\delta - \frac{d\delta^*}{dx}. \tag{5}$$

Webb *et al.* found it convenient to introduce the following transformation for the spatial coordinates x and y:

$$\begin{aligned} \xi(x) &= R_\infty^{-1} \int_0^x \frac{\rho_\delta u_\delta}{\mu_\delta}\, dx \\ \eta(x, y) &= \frac{\rho_\delta u_\delta}{R_\infty \mu_\delta} \int_0^y \frac{\rho}{\rho_\delta}\, dy. \end{aligned} \tag{6}$$

Furthermore, a dimensionless velocity, $U = u/u_\delta$, was adopted. Equation (2) then becomes

$$f_\eta f_{\xi\eta} - f_\xi f_{\eta\eta} - [(1-f_\eta^2) - 2(1-\varepsilon)ff_{\eta\eta}]\beta - \frac{1}{R_\infty} f_{\eta\eta\eta} = 0 \tag{7}$$

where $f = \int_0^\eta U\, d\eta$ and $\beta = -\dfrac{1}{2\varepsilon(1-\varepsilon)}\dfrac{d\varepsilon}{d\xi}$.

We now define the i-th moment of the x-momentum equation (2) by the integral relation

$$\int_0^{\eta_\delta} f_\eta^i [\text{left side of Equation 7}]\, d\eta = 0. \tag{8}$$

For the moment integrals the normalized polynomial velocity profiles of [4] are considered:

$$U = 1 - (1 - U_0) S(v) \tag{9}$$

where

$S(v) = 1 - 2v^2 + v^4$ when a quartic profile is desired

$S(v) = 1 - 3v^2 + 2v^3$ when a cubic profile is desired

and

$$v = \frac{\eta}{\eta_\delta} \text{ where } 0 < v < 1. \tag{10}$$

It may be noted that these profiles satisfy the zero-gradient condition at the axis $[(\eta/\eta_\delta) = 0]$ and at the edge of the shear layer $[(\eta/\eta_\delta) = 1]$. U_0, η_δ and ε are unknown functions of ξ. To solve for these quantities, one finds three first-order simultaneous ordinary differential equations

by means of the overall continuity equation (5), and the zero-th and first moments of the momentum relation (8). In order to write the equations simply, one may adopt the following shorthand notation: $x_1=\varepsilon$, $x_2=U_0$ and $x_3=\eta_\delta R_\infty$. The symbols x_1, x_2, x_3 and $\varepsilon, U_0, \eta_\delta R_\infty$ will be used henceforth interchangeably. One further writes for the independent variable $\zeta=\xi R_\infty$, so that R_∞ no longer appears explicitly in the differential equations. The implication of this substitution will be discussed later.

The three first-order simultaneous differential equations can now be written compactly:

$$a_{ij}\dot{x}_j = C_i \qquad (i,j=1,2,3) \tag{11}$$

where the coefficients a_{ij} and C_i are functions of x_j; the dot signifies total differentiation with respect to ζ. Explicit expressions for these coefficients are given in the Appendix.

The derivative of each component x_i can be obtained by Cramer's rule so that Eq. (11) becomes symbolically

$$\frac{dx_i}{N_i(x_j)} = \frac{d\zeta}{D(x_j)} \tag{12}$$

where D is the determinant of the matrix $\{a_{ij}\}$.

3. Analysis of the Singularities

Equation (12) is invariant under translation of the independent variable ζ; such a set is known as an autonomous system. It is possible to exploit the translational invariance and to obtain by division two equations of the form

$$\frac{dx_1}{dx_2} = \frac{N_1(x_1,x_2,x_3)}{N_2(x_1,x_2,x_3)}$$

and (13)

$$\frac{dx_3}{dx_2} = \frac{N_3(x_1,x_2,x_3)}{N_2(x_1,x_2,x_3)}.$$

The variables x_1, x_2, x_3 form a three-dimensional space (called the Poincaré phase space [6, 7]).

A point x_{1c}, x_{2c}, x_{3c} in the phase space for which $N_i(x_{jc})=0$, $i,j=1,2,3$ is called a singular point or singularity of (13). It can be shown that $D(x_{1c}, x_{2c}, x_{3c})$ in (12) must then also be equal to zero. Equation (12) is then said to have a singular point in the ζ-plane. However, its location in ζ is not known until further computation (discussed below) is carried out. Near the singular point, $N_i(x_j)$ can be expressed by a Taylor series:

$$N_i(x_j) = C_{ij}(x_j - x_{jc}) + O[(x_j - x_{jc})^2] \tag{14}$$

where the coefficients C_{ij} are obtained by evaluating the first partial derivatives $\partial N_i/\partial x_j$ at $x_j=x_{jc}$. The behavior of the integral curves of (13) in the neighborhood of the singular point* depends entirely on these coefficients. It is known from classical analyses in phase space that if one forms a cubic algebraic equation in λ from the C_{ij} of the type:

$$|C_{ij}-\lambda\delta_{ij}| = 0\,, \qquad \delta_{ij} = \begin{cases} 1 & i=j \\ 0 & i\neq j \end{cases} \tag{15}$$

then the values of the roots, $\lambda_k\,(k=1,2,3)$ of (15) determine the type of singularity at $x_j=x_{jc}$ [6].

In the particular application of Poincaré phase space analysis to the near wake, each N_i in Eq. (13) is set to zero:

$$N_i(x_1,x_2,x_3) = 0\,, \qquad i=1,2,3 \tag{16}$$

Geometrically, each N_i represents a surface in phase space. In the interval $-1<U_0<1$, only two independent relations can be derived from Eqs. (16). This indicates that the intersection of

* Higher-order singularities are not considered here.

the three surfaces are curves rather than points. The two relations are here formally written:

$$F_1(x_1, x_2) = 0 \tag{17a}$$

and

$$F_2(x_1, x_2) = x_3 \tag{17b}$$

Full expressions of N_i, F_1, F_2 and $\partial N_i/\partial x_j$ are given in the Appendix.

The solution of Equation (17a), which depends only on the assigned velocity profile, yields curves in the (x_1, x_2) plane. These curves are here called the base curves. In Fig. (2a), the base curve based upon the quartic profile is presented, while in Fig. (2b) two base curves, one based upon the quartic and the other based upon the cubic profile, are shown in the range $0.3 < x_2 < 0.35$ to illustrate the influence of the chosen velocity profiles. Upon specification of a freestream Mach number*, the location of the singularities (curves in phase space) can be determined from

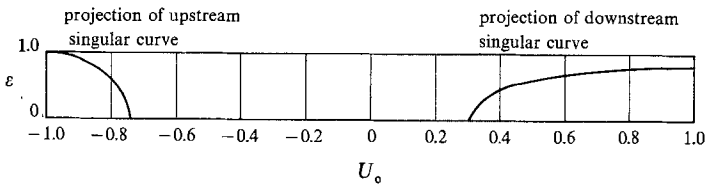

Fig. 2a. Base curves or projection of singular curves on the (ε, U_0) plane for a quartic profile.

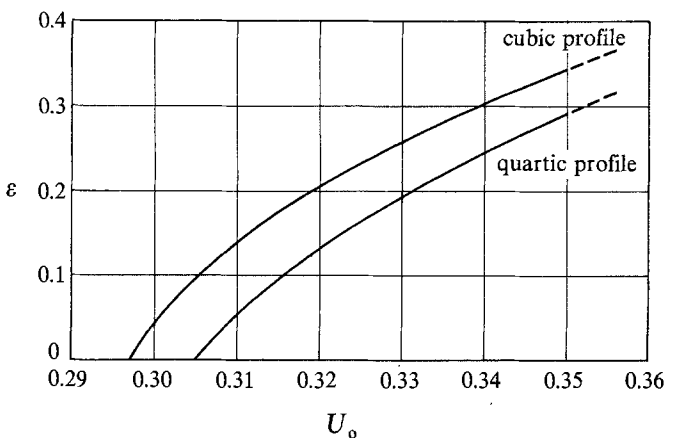

Fig. 2b. Enlarged section of base curves for $0.3 < U_0 < 0.35$ for both cubic and quartic profiles.

Eq. (17b) by substitution into F_2 of the values of x_1 and x_2 found from Eq. (17a). The form of Eq. (17b) suggests that the base curves are just the projections of the singular curves on the (x_1, x_2) or (ε, U_0) plane. A one-to-one correspondence exists between the points on the base curves and the singular curves.

Equation (17) is also satisfied by the point $\varepsilon = \varepsilon_\infty = \{1 + \frac{1}{2}(\gamma - 1)M_\infty^2\}^{-1}$, $U_0 = 1$ and $x_3^{-1} = 0$. One notices that this singular point in phase space corresponds to the freestream condition of the flow.

Having located all the singularities, one now proceeds to study the nature of each singular point.

1. The downstream singular curve ($U_{0_c} > 0$). With reference to Fig. 3, for points on the singular curve with values of ε in the range, $\varepsilon_\infty > \varepsilon \geqq \varepsilon_l$, Eq. (15) yields three real roots; one root is positive,

* The specification of the freestream Mach number M_∞ establishes an asymptote, i.e., an upper limit, for ε, called ε_∞. The condition $\varepsilon_\infty \geqq \varepsilon > 0$ implies that $\phi \geqq 0$.

one negative and one very close to zero. Because these roots are purely real and because roots with both positive and negative signs occur, it is well-known from phase plane theory that these singularities are saddle points. For those points on the singular curve with values of $\varepsilon < \varepsilon_l$, Eq. (15) yields one real root very close to zero and two conjugate complex roots. Such singularities are either focal of saddle-foci. The singularities are focal points if the signs of the purely real root and of the real part of the complex roots are the same; if not, the singularities are saddle-foci. As the freestream Mach number is increased, the band of saddle points contracts. The bands of saddle points are shown (on base curves) in Fig. 3 for $M_\infty = 6$ and 10.

2. The upstream singular curve ($U_{0_c} < 0$). Saddle points are found on this curve. These saddle points are in the reversed flow region because $U_{0_c} < 0$. The local Mach number associated with these saddle points is too high to be physically acceptable for the reverse flow region, known

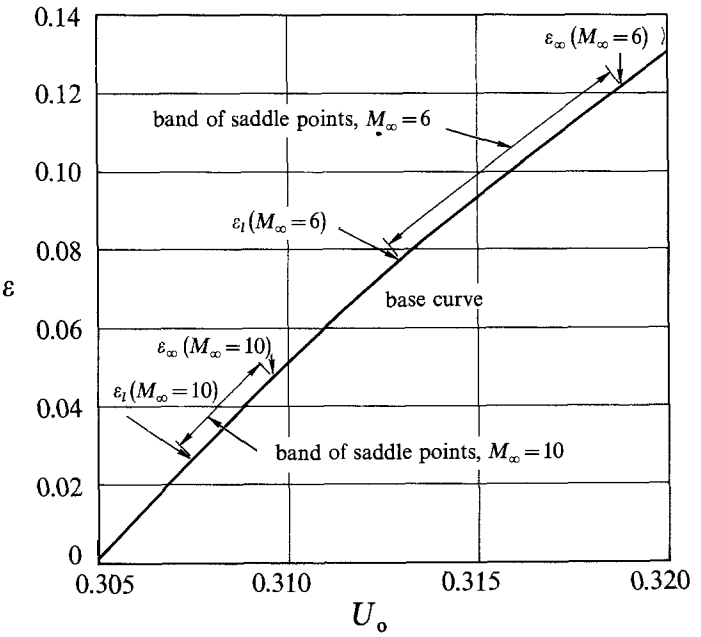

Fig. 3. Projection of bands of saddle points for $M_\infty = 6$, 10 for a quartic profile.

from experiments* to be characterized by small Mach number. Hence, these singularities can have no relevance to the nearwake problem.

3. The freestream condition. At this singular point, all first partial derivatives vanish. Consequently, this point is a singularity of higher order.

As mentioned earlier, R_∞ does not appear explicitly in the differential equations. Thus, the locations as well as the nature of the singularities are independent of this parameter. This observation saves a great deal of work when the equations are integrated. Specifically, rather than having a two-parameter (M_∞, R_∞) family of solutions (as was the case in [4]), one deals with a one-parameter (M_∞) family of solutions.

4. Integration of the Equations

The remaining task is to obtain those integral curves which pass through the downstream saddle points. Since the saddle point is known to be unstable as far as numerical integration is concerned, it is always easier to integrate away from a saddle point rather than toward it [8].

* Private communication with Dr. Richard G. Batt of TRW Systems.

In order to integrate away from the singular point, one must determine the slopes of the integral curves at the singularity. In three-dimensional phase space, the characteristic equation (15) has three distinct real roots. λ_1 is taken as the positive root; $\lambda_2 \approx 0$; and λ_3 is the negative root. Each root yields a set of values of the slopes dx_1/dx_2 and dx_3/dx_2. Hence three distinct integral curves go through each saddle point. Once the values of dx_1/dx_2 and dx_3/dx_2 are found at the saddle point, the derivatives $dx_i/d\zeta$ at the singular point in physical space can also be determined in a similar process in which the determinant D in (12) is expanded in a Taylor series. A typical example of the initial slopes dx_1/dx_2 or $d\varepsilon/dU_0$ is presented in Fig. 4. The first positive slope is associated with the positive characteristic root λ_1; the negative slope, with the negative root λ_3; and the second positive slope, with the slope $\lambda_2 \approx 0$. One notices that the second positive slope (exaggerated in the drawing) is almost tangent to the base curve. This is not surprising since the slope of the base curve corresponds to a zero root. This fact indicates that the curvature terms (second derivatives) play an important role on this integral curve.

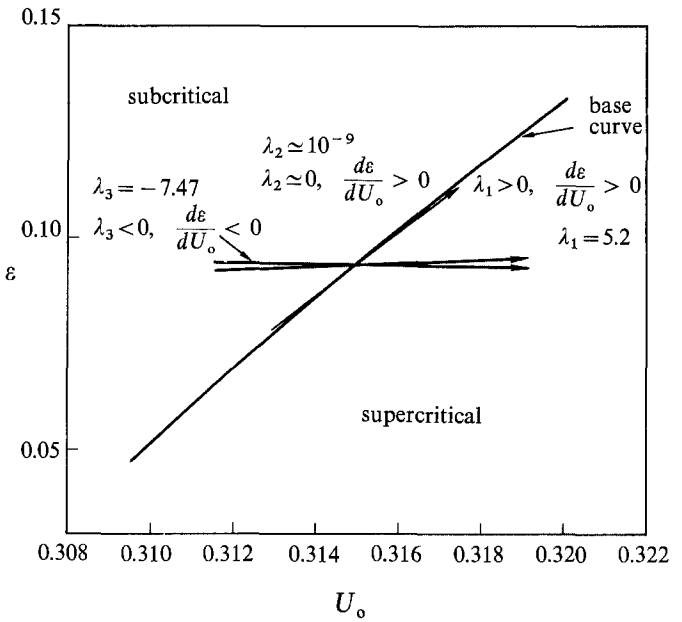

Fig. 4. Initial slopes, $d\varepsilon/dU_0$, at a saddle point for $M_\infty = 6$, quartic profile.

Either Eq. (13) or (12) can now be integrated to give the final answer. Equation (12), however, has the advantage of also yielding the corresponding physical distance.

One must now decide which characteristic root yields the wake solution. Based on physical considerations, one adopts the following criteria to select the wake solution:

(1) The integral curve in phase space must go through the rear stagnation plane ($U_0 = 0$) and the saddle point ($0 < U_{0_c} < 1$), and must approach the freestream condition asymptotically.

(2) Along the integral curve, one requires that $d\varepsilon/dU_0 > 0, \eta_\delta > 0$ and $\varepsilon_\infty > \varepsilon > 0$. The condition $d\varepsilon/dU_0 > 0$ implies that $d\varepsilon/d\zeta > 0$ and $dU_0/d\zeta > 0$ in physical space

(3) Integration through the saddle point must move a point on the integral curve from the subcritical region to the supercritical region.

This three-part criterion immediately picks the positive root λ_1 as the right one. The integral curves calculated from the two remaining characteristic roots also provide mathematically correct solutions to the differential equations, but are not physically acceptable as descriptions of the wake.

5. Results and Conclusions

As mentioned earlier, for a given freestream Mach number, the downstream singular curve consists of a band of saddle points, from each of which stem integral curves. Integration from all the saddle points provides, therefore, an infinite number of integral curves or a continuous integral surface (see Fig. 5). Proceeding downstream, one finds that the numerical process is very stable and all the integral curves converge asymptotically to the freestream condition ($U_0 \to 1, \varepsilon \to \varepsilon_\infty$ as $\eta_\delta \to \infty, \zeta$ or $x \to \infty$). Based on this fact, one concludes that the point corresponding to the freestream condition behaves like a node. Proceeding upstream, however, one discovers that the situation is somewhat different. Since the rear stagnation point is a regular point of the differential equations, integral curves from different saddle points would lead to different rear stagnation points on the $U_0 = 0$ plane, and the loci of these rear stagnation points, which is the intersection of the integral surface and $U_0 = 0$ plane, is a continuous curve (see Fig.

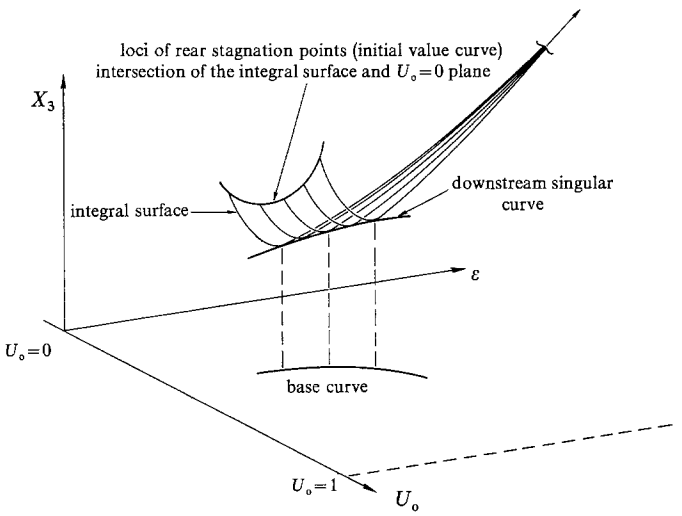

Fig. 5. Sketch of the integral curves through the downstream saddle points in phase space.

5). This curve, called the initial value curve, is presented in two different ways in Fig. 6. In Fig. 6a, the curve is plotted with x_3 as the ordinate and U_{0_c} as the abscissa; hence one knows from which saddle point the integral curve comes. In Figure 6b, ε_i replaces U_{0_c} as the abscissa and ε_i is the value of ε which corresponds to the rear stagnation point. The curve shown in Fig. 6 is a universal one for a given M_∞.

The location of the singularity in the physical plane, ζ-plane, can now be found. Denoting ζ_c as the distance between the singularity and the rear stagnation point, one determines this distance when the integration of Eq. (12) which starts from $U_0 = U_{0_c}$ and $\zeta = \zeta_c$, reaches a value of $U_0 = 0$ (which corresponds to $\zeta = 0$). This singularity is the Crocco–Lees critical point.

In order to bring out the effect of the freestream Reynolds number, one must know the physical shear layer thickness δ_i. From the definitions of $\eta(x, y)$ and x_3, δ_i can be calculated once R_∞ is specified. As an example, for $M_\infty = 6$ and $R_\infty = 10^5$, values of δ_i are calculated and the results are given in Fig. 7a and 7b. One notices that by specifying different R_∞, the curves in Fig. 7 merely move up (R_∞ decreasing) or down (R_∞ increasing). It is not difficult to understand certain numerical discoveries of Drs. W. Webb and R. Golik (private communication). The lowest point of the curve corresponds to the case $R_\infty = R_{\infty_m}$. Above this point there are always two points on the curve corresponding to the same value of δ_i; thus two acceptable initial conditions appear. Furthermore, in [4], the value of δ_i is always taken to be unity and, based on this length, R_∞ is defined. In the present calculation, if R_∞ is defined based on an unspecified length of value unity, then the value of δ_i can no longer be specified at will but must be accepted from the calculations. We may, however, introduce an equivalent Reynolds

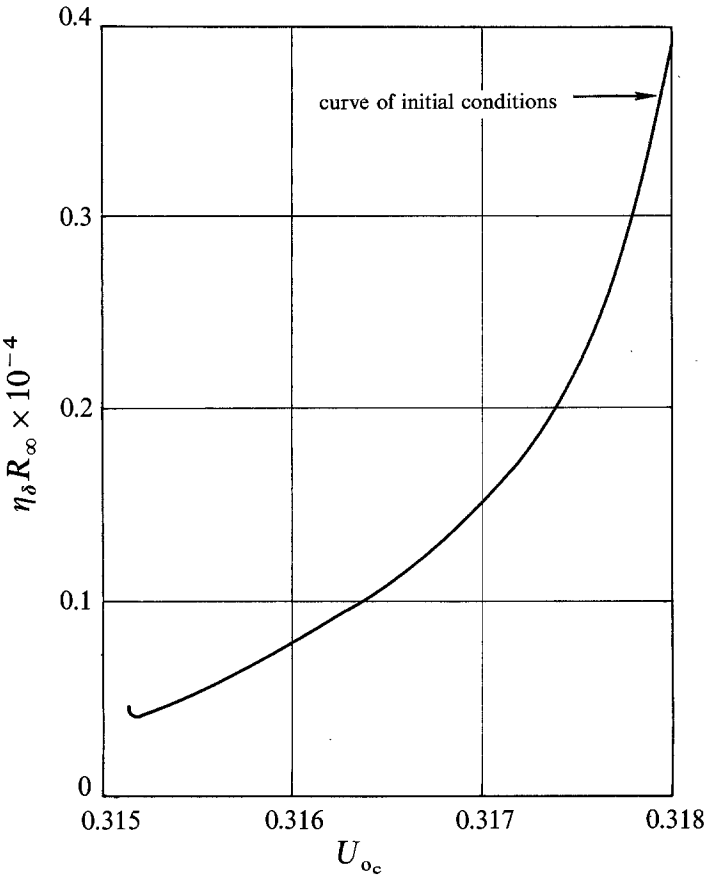

Fig. 6a. x_3 *versus* U_{o_c} in the $U_o=0$ plane. $M_\infty=6$.

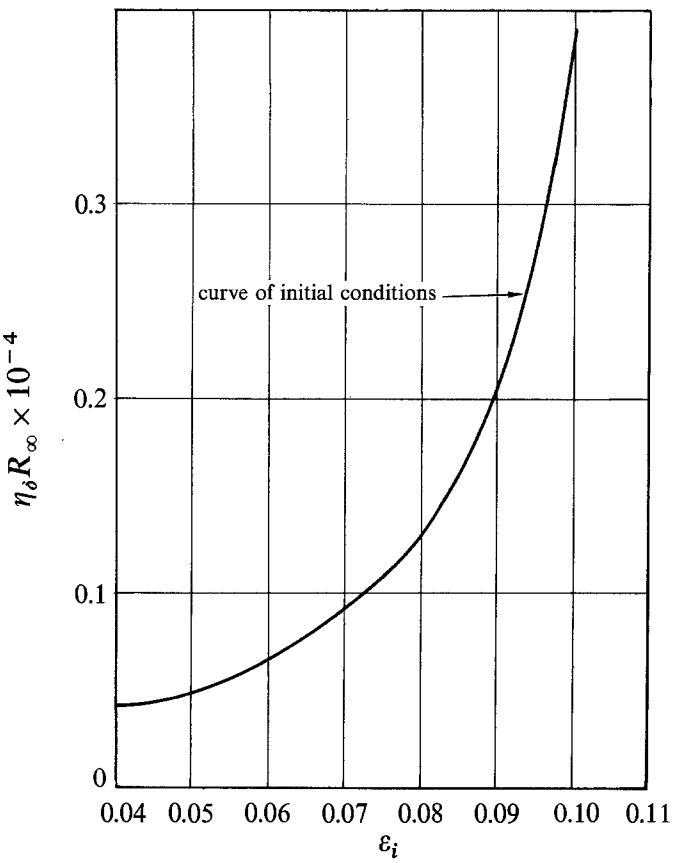

Fig. 6b. x_3 *versus* ε_i in the $U_o=0$ plane. $M_\infty=0$.

number R_{∞_e} based on the calculated values of δ_i. The relation between the two Reynolds numbers is obviously just $R_{\infty_e} = \delta_i \times R_\infty$. Taking $\delta_i = 0.2$ from the lowest point of the curve in Fig. 7, one obtains $R_{\infty_e} = 2 \times 10^4$. This is exactly the value of R_{∞_m} found by Webb and Golik, as mentioned in the Introduction. Hence, their result is explained. Different saddle points on the singular curve are associated with different Reynolds numbers.

Integration from the saddle points upstream does not necessarily bring the integral curve through the rear stagnation point. Calculations show that for the case of $M_\infty = 6$, at a value of

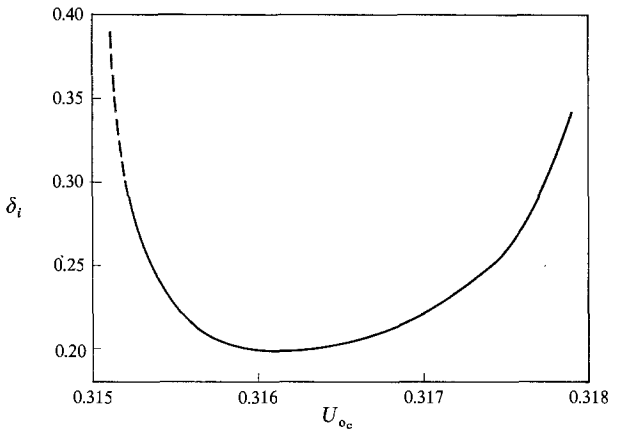

Fig. 7a. Initial value curve in the rear stagnation plane ($U_o = 0$). $M_\infty = 6$, $R_\infty = 10^5$, quartic profile.

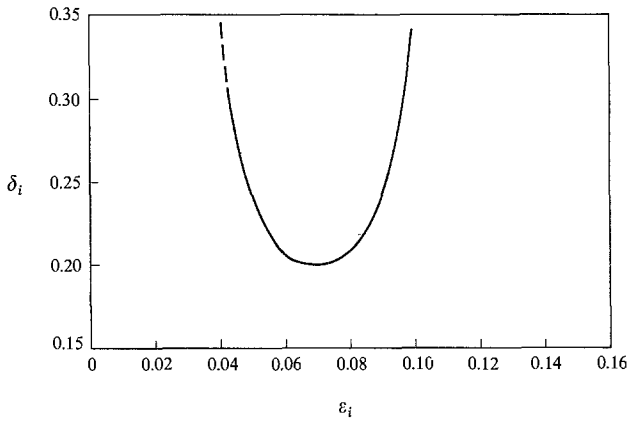

Fig. 7b. Initial value curve in the rear stagnation plane ($U_o = 0$). $M_\infty = 6$, $R_\infty = 10^5$, quartic profile.

$U_{o_c} = 0.3151$, the integral curve ceases to cross $U_o = 0$, even though saddle points exist at values of U_{o_c} as low as 0.313 (Fig. 3). As an illustration of this observation, two typical integral curves of U_o *vs.* x are drawn in Fig. 8. In Fig. 8a, the integration starts from the saddle point corresponding to $U_{o_c} = 0.315$ and the curve never reaches a $U_o = 0$ condition. Based on this fact, the conclusion is drawn that not all of the saddle points are critical points of the wake solution.

We now summarize our findings in the following:

1. Two singular lines exist in the phase space, one upstream and one downstream of the rear stagnation point. The upstream one has no physical meaning to the near wake flow, while the downstream one consists of saddle points.
2. The point at downstream infinity is a singularity of higher order; it behaves like a node.
3. Three integral curves pass through each saddle point on the downstream singular curve in phase space. The wake solution corresponds to the one associated with the positive characteristic root. Not all of the saddle points yield a wake solution. Those saddle points

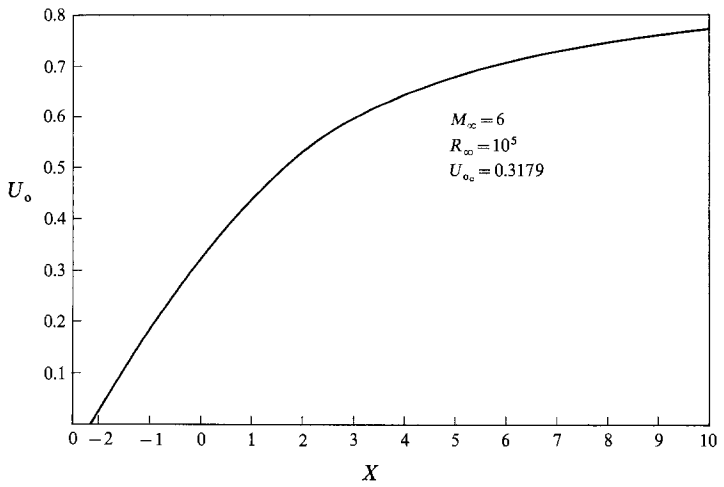

Fig. 8a. Wake solution.

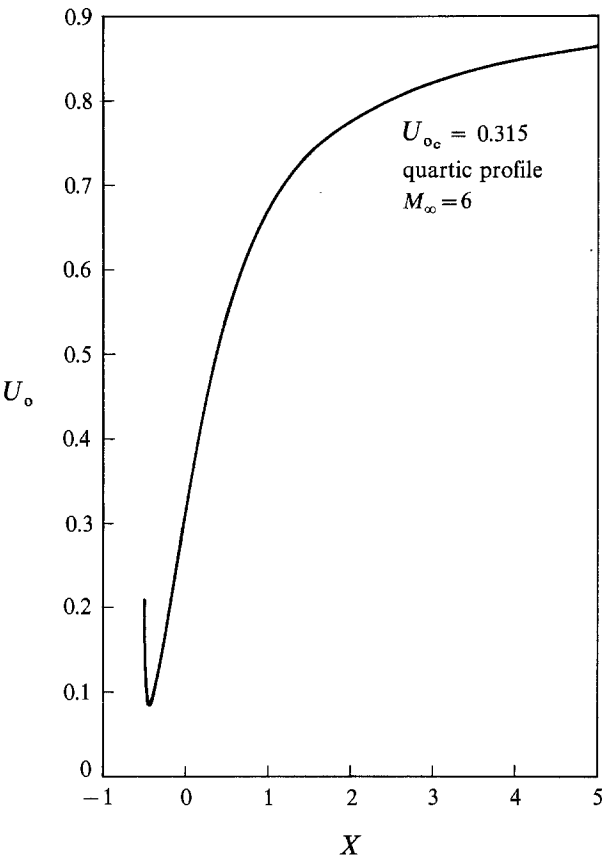

Fig. 8b. Non-wake solution.

which do lead to wake solutions correspond to the Crocco–Lees critical points in the physical plane.

4. The differential equations yield a one-parameter (M_∞) family of solution instead of a two-parameter family (M_∞, R_∞) as suggested in the work of Webb *et al.* The effect of the Reynolds number (R_∞) comes in only at the initial condition.
5. The existence of a minimum freestream Reynolds number and of the double initial conditions found by Webb and Golik has been clarified.

These phenomena demonstrate the limitation of the multimoment method for wake calculations, since for freestream Reynolds number below a certain minimum, no solution can be furnished by the method. Furthermore, the theory itself provides no way to choose the right branch of solution for $R_{\infty_e} > R_{\infty_m}$ unless additional information is given.

Acknowledgement

The author wishes to express his sincere thanks to Professors Lester Lees and Toshi Kubota of Caltech, to Professor George F. Carrier of Harvard University, his colleague Dr. Francis E. Fendell of TRW Systems, and to Mr. Daniel Ko of Caltech, who assisted with the numerical work.

Appendix

In this appendix the full expressions of many quantities treated symbolically in the text are given. The a_{ij} and C_i of Eq. (11), $N_i(x_j)$ and $D(x_j)$ of Eq. (12), F_1 of Eq. (17a), F_2 of Eq. (17b) and the first order partial derivative $\partial N_i/\partial x_j$ are for the present case:

$$a_{ij} = \begin{Bmatrix} \varepsilon^* \psi^{-1} R_\infty & -Ax_3 & AW \\ -\varepsilon^* \Delta^* R_\infty & K_1 x_3 & K_2 W \\ -2\varepsilon^* \varepsilon \theta_1 R_\infty & K_3 x_3 & K_4 W \end{Bmatrix}, \qquad C_i = \begin{Bmatrix} -\varepsilon\phi \\ 0 \\ 2\dfrac{W^2}{x_3} G \end{Bmatrix}$$

where

$$W = 1 - U_0, \quad A = \int_0^1 S^2(v)\,dv, \quad B = \int_0^1 S^2(v)\,dv$$

$$C = \int_0^1 S^3(v)\,dv, \quad G = \int_0^1 \left(\frac{\partial S}{\partial v}\right)^2 dv, \quad \varepsilon^* = \tfrac{1}{2}[\varepsilon(1-\varepsilon)]^{-1}$$

$$\psi^{-1} R_\infty = \bar{\psi} = x_3(A^*\varepsilon^2 + B^*\varepsilon + C^*) \qquad \Delta^* R_\infty = \bar{\Delta} = x_3 W(WB + 2K_2\varepsilon)$$

$$\theta_1 R_\infty = \bar{\theta}_1 = x_3 W K_4$$

$$\frac{\partial N_1}{\partial x_1} = -Wx_3(K_1K_4 - K_2K_3)\left(\phi + \varepsilon\frac{d\phi}{d\varepsilon}\right)$$

$$\frac{\partial N_1}{\partial x_2} = x_3\varepsilon\phi\left[(K_1K_4 - K_2K_3) - ABW\left(1 - 4\frac{C}{B}W + 3\frac{C}{A}W^2\right)\right] + 8ABGW^3$$

$$\frac{\partial N_1}{\partial x_3} = -W\varepsilon\phi(K_1K_4 - K_2K_3)$$

$$\frac{\partial N_2}{\partial x_1} = -Bx_3W^3K_4\varepsilon^*\left(\phi + \varepsilon\frac{d\phi}{d\varepsilon}\right) - 2G\varepsilon^*W^3K_2(2A^*\varepsilon + B^* + 2AW)$$

$$\begin{aligned}\frac{\partial N_2}{\partial x_2} = {} & Bx_3W^2[3K_4 + W(2WC - 3B)]\varepsilon^* e\phi + \\ & + 6\varepsilon^* GW^2[K_2A^*\varepsilon^2 + K_2(B^* + 2AW)\varepsilon + K_2C^* + ABW^2] \\ & + 2\varepsilon^* W^3 G\left[\varepsilon^2\frac{d}{dW}(K_2A^*) + \varepsilon\frac{d}{dW}(K_2(B^* + 2AW)) + \frac{d}{dW}(K_2C^* + ABW^2)\right]\end{aligned}$$

$$\frac{\partial N_2}{\partial x_3} = -BW^3K_4\varepsilon^*\varepsilon\phi$$

$$\frac{\partial N_3}{\partial x_1} = x_3^2 W\varepsilon^*(K_3 WB - 2K_5\varepsilon)\left(\phi+\varepsilon\frac{d\phi}{d\varepsilon}\right)+$$
$$-2x_3^2\varepsilon^*\varepsilon\phi WK_5+2W^2G\varepsilon^*x_3(2K_1A^*\varepsilon+K_1B^*-2K_2AW)$$
$$\frac{\partial N_3}{\partial x_2} = -x_3^2\varepsilon^*\varepsilon\phi W\left[B\frac{d}{dW}(K_3W)+2\varepsilon AB\left(1-4\frac{C}{B}W+3\frac{C}{A}W^2\right)\right]$$
$$-2WG\varepsilon^*x_3[K_1A^*\varepsilon^2+(K_1B^*-2K_2AW)\varepsilon+K_1C^*-ABW^2]+$$
$$-2W^2G\varepsilon^*x_3\left[\varepsilon^2\frac{d}{dW}(K_1A^*)+\varepsilon\frac{d}{dW}(K_1B^*-2K_2AW)+\frac{d}{dW}(K_1C^*-ABW^2)\right]$$
$$\frac{\partial N_3}{\partial x_3} = x_3\varepsilon^*\varepsilon\phi W[K_3WB-2K_5\varepsilon].$$

$$A^* = \frac{\gamma+1}{\gamma-1}(1-2WA+W^2B)$$
$$B^* = \frac{\gamma+1}{\gamma-1}(2AW-W^2B)-\frac{2}{\gamma-1}(1-2WA+W^2B)-W^2B$$
$$C^* = W^2B-\frac{2}{\gamma-1}(2AW-W^2B)$$

$$K_1 = -A+2WB \qquad K_2 = A-WB \qquad K_3 = -2A+6WB-3W^2C$$
$$K_4 = 2A-3WB+W^2C \qquad K_5 = K_1K_4-K_2K_3$$
$$N_1 = N_\varepsilon = -x_2W[K_5\varepsilon\phi+A(K_1+K_2)\theta_2^*]$$
$$N_2 = N_{v_0} = \varepsilon^*W[2K_2\varepsilon^2\phi\bar{\theta},-A\theta_2^*\bar{\Delta}-K_4\varepsilon\phi\bar{\Delta}-K_2\theta_2^*\bar{\psi}]$$
$$N_3 = \varepsilon^*x_3[K_1\theta_2^*\bar{\psi}+K_3\bar{\Delta}\varepsilon\phi-2K_1\varepsilon_2\phi\bar{\theta}_1-A\theta_2^*\bar{\Delta}]$$
$$D = \varepsilon^*Wx_3[K_5\bar{\psi}+2ABW\varepsilon\bar{\theta}_1-AW(3B-2WC)\bar{\Delta}]$$
$$F_1(\varepsilon,U_0) = [2\varepsilon W(K_1K_4-K_2K_3)-K_3W^2B]+$$
$$+\left(1-2\frac{C}{B}W+\frac{C}{A}W^2\right)[K_1(A^*\varepsilon^2+B^*\varepsilon+C^*)-AW(WB+2K_2\varepsilon)] = 0, \quad (17a)$$

$$F_2(\varepsilon, U_0) = \frac{2GW^2}{\varepsilon\phi\left(1-2\frac{C}{B}W+\frac{C}{A}W^2\right)} = x_3 \quad (17b)$$

REFERENCES

[1] L. Crocco and L. Lees, A Mixing Theory for the Interaction between Dissipative Flows and Nearly Isentropic Streams, *J. Aero. Sci.*, 19 (1952) 649–676.

[2] B. L. Reeves and L. Lees, Theory of the Laminar Near Wake of Blunt Bodies in Hypersonic Flow, *AIAA J.*, 3, 11 (1965) 2061–2074.

[3] K. Stewartson, Further Solutions of the Falkner-Skan Equation, *Proc. Cambridge Phil. Soc.*, 50 (1954) 454–465.

[4] W. H. Webb, R. J. Golik, F. W. Vogenitz and L. Lees, A Multimoment Integral Theory for the Laminar Supersonic Near Wake, *Proceedings of the 1965 Heat Transfer and Fluid Mechanics Institute*, Stanford University Press, 1965, pp. 168–189.

[5] E. Baum and M. R. Denison, Interaction Supersonic Laminar Wake Calculations by a Finite Difference Method, *AIAA J.*, 5 (1967) 1224–1230.

[6] H. Poincaré, Sur les Courbes de Finie par les Equations Différentielles, *J. Math.*, 4–2, 1886, 151–217.

[7] H. Poincaré, *Oeuvres*, Vol. 1, Gauthier-Villars, Paris, 1928.

[8] D. Gilbarg and D. Paolucci, The structure of Shock Waves in the Continuum Theory of Fluids, *J. Rat. Mech. Anal.*, 2 (1953) 617–642.